

# INFLUENȚA GHIPSULUI, ROCĂ NATURALĂ SAU DEȘEU INDUSTRIAL, ASUPRA PROPRIETĂȚILOR MORTARELOR DE CIMENT PORTLAND

## INFLUENCE OF GYPSUM, AS NATURAL ROCK OR INDUSTRIAL WASTE, ON THE PROPERTIES OF PORTLAND CEMENT MORTARS

RĂZVAN LISNIC<sup>1,2</sup>, CRISTINA BUSUIOC<sup>1\*</sup>, GEORGETA VOICU<sup>1</sup>, SORIN-ION JINGA<sup>1</sup>

<sup>1</sup> University POLITEHNICA of Bucharest, RO-011061, Bucharest, Romania

<sup>2</sup> S.C. CEPROCIM S.A., RO-062203, Bucharest, Romania

Two types of natural gypsum from different regions of Romania and two types of synthetic gypsum resulted in the flue gas desulfurization (FGD) industrial installation where characterized from compositional, structural and morphological point of view by thermal analysis, X-ray diffraction, scanning electron microscopy coupled with energy dispersive X-ray spectroscopy and laser granulometry. The mortars developed based on portland cement and different proportions of gypsum were also investigated in terms of setting time and mechanical properties (flexural strength and compression strength), in correlation with the visualization of the hydration products through scanning electron microscopy. The results were correlated with the purity and homogeneity of the analysed gypsum specimens.

Două tipuri de ghips natural prelevate din regiuni diferite ale României și două tipuri de ghips sintetic provenite din instalațiile industriale de desulfurare a gazelor de ardere au fost caracterizate din punct de vedere compozițional, structural și morfologic prin analiză termică, difracție de raze X, microscopie electronică cu baleiaj cuplată cu spectroscopie de raze X cu dispersie după energie și granulometrie laser. Mortarele obținute pe bază de ciment portland și diferite proporții de ghips au fost, de asemenea, investigate din punctul de vedere al timpului de priză și al proprietăților mecanice (rezistență la încovoiere și rezistență la compresiune), în corelare cu evidențierea produșilor de hidratare prin microscopie electronică cu baleiaj. Rezultatele au fost corelate cu puritatea și omogenitatea specimenelor de ghips analizate.

**Keywords:** Portland cement; Natural gypsum; FGD gypsum; Setting time; Flexural strength; Compression strength.

### 1. Introduction

Coal combustion products [1] are materials produced when coal is burned to generate electricity. Power plants equipped with flue gas desulfurization (FGD) [2, 3] emissions control systems, also known as scrubbers, create by-products that include synthetic gypsum. Scrubbers utilize high-calcium reagents [4], such as lime or limestone, to capture sulphur dioxide from the flue gases. Synthetic gypsum is one of the by-products of "clean coal" technologies.

Sulphur dioxide is a major contributor to "acid rain" formation, so creating a market for synthetic gypsum benefits everyone. The use of synthetic gypsum in construction materials industry [5-9] avoids the mining of virgin gypsum, yielding water, energy and emissions reductions.

In order to tackle waste production, waste needs to be diverted from incineration and landfill to reduce environmental pollution and create a more sustainable and circular economy. One proven solution to reducing the impact of waste is to transform waste into recycled materials and thermal energy in cement manufacturing.

The current paper presents a comparison between types of portland cement to which they

have been used as a setting retarder: two samples of synthetic gypsum obtained from desulphurisation of combustion gases and two samples of natural gypsum. To have a better overall view of the four portland cement mortars, the gypsum samples were dosed in proportions from 1 to 5 % in addition to the industrial clinker.

### 2. Experimental

In this study, the following materials and codifications were used: GB - natural gypsum sample 1, GT - natural gypsum sample 2, GG - synthetic gypsum sample 1, GR - synthetic gypsum sample 2, as well as industrial clinker. The synthetic gypsum samples, in the form of sludge, after water removal were dried in a drying chamber at 40 °C. The drying was done at this temperature in order to avoid the transformation of gypsum into anhydrite.

The same clinker was employed for all cements, with the mineralogical composition given in Table 1.

Type CEM I cements, according to [10], were done through simultaneous grinding of the components. Grinding was done in two steps. In the first step, preliminary ball milling of clinker took

\* Autor corespondent/Corresponding author,  
E-mail: [cristina.busuioc@upb.ro](mailto:cristina.busuioc@upb.ro)

**Table 1**

Mineralogical composition of the clinker  
Compoziția mineralogică a clinkerului.

No.	Phase	Proportion (%)
1	Alite	67.72
2	Belite	12.66
3	Celite	8.77
4	Tricalcium aluminate	7.30
5	Lime	1.34
6	Portlandite	0.32
7	Periclase	0.42
8	Aphthitalite	0.84
9	Arcanite	0.61

place up to a fineness expressed as  $R_{009}$  of approximately 40 %. Taking into consideration that synthetic gypsum was characterized by an advanced fineness, this was added to grinding in the finishing step, to ensure an appropriate cement homogenization and a reduced energy consumption; a final Blaine specific surface area of about 3,250 cm<sup>2</sup>/g was achieved with a tubular laboratory mill with double bevelled cones.

A Shimadzu DTG-60 equipment was employed to perform the thermal analysis, in the 25 - 1000 °C temperature range. The crystalline features of the samples were analyzed by X-ray diffraction (XRD), using a Shimadzu XRD 6000 diffractometer with Ni filtered Cu K $\alpha$  radiation ( $\lambda = 0.154$  nm),  $2\theta$  ranging between 10 and 80 °. The morphology and elemental composition of the samples were determined through scanning electron microscopy (SEM) coupled with energy-dispersive X-ray spectroscopy (EDX), employing a FEI Quanta Inspect F scanning electron microscope; the specimens for SEM analysis were covered with a thin gold layer deposited by DC sputtering. A Malvern Mastersizer 2000 laser diffraction particle size analyzer was used to evaluate the particle size distribution in air. SO<sub>3</sub> content of cements was determined in accordance with the method presented in SR EN 196-2:2013 [11].

In order to evaluate the binding properties (setting time on paste, flexural strength and compressive strength) of the mortars based on portland cement and five concentrations of gypsum as additive for inhibiting hydration and delaying setting (retarder), testing samples were prepared by following SR EN 196-3:2017 standard [12] for the setting time measurement and SR EN 196-1:2016 standard [13] for the strengths determination.

### 3.Results and discussion

In order to study the dehydration process of gypsum, the powders were subjected to a thermal analysis from room temperature to 1000 °C, in air (Fig. 1). The thermogravimetric curves (Fig. 1a) highlight two stages of weight loss, the first one between 60 and 230 °C and the second one in the 610 - 760 °C temperature range. The main endothermic process corresponds to a double

peak effect and can be assigned to the dehydration of gypsum dehydrate to hemihydrate and then to anhydrite [14]. The secondary process (610 - 760 °C) is also an endothermic one, but with a much lower calorific effect, being caused probably by the decomposition of attendant calcium carbonate at higher temperatures. Moreover, a small exothermic effect can be seen between 340 and 430 °C (Fig. 1b); this can be attributed to a polymorph transition of calcium sulfate, from CaSO<sub>4</sub> III to CaSO<sub>4</sub> II, forms with different reactivity with respect to water [15].

Considering the aspect of the curves, the four samples can be divided into two groups: GB and GT, with a significant weight loss around 700 °C, and GG and GR, with a reduced weight loss at the mentioned temperature, but also a higher heat consumption for the main process. This behaviour is strongly related to the degree of contamination of the raw materials with other minerals, these shifting the thermal processes at lower or higher temperatures and also influencing their intensity.

Moreover, it can be observed that the endothermic effect placed in the 60 - 230 °C temperature range is more intense for GG and GR than GB and GT, which may suggest a higher content of SO<sub>3</sub>; as well, the maximum temperature of this effect decreases in the series GG-GB-GR-GT, fact that can be correlated with the decrease of crystallinity degree and/or increase of fineness.

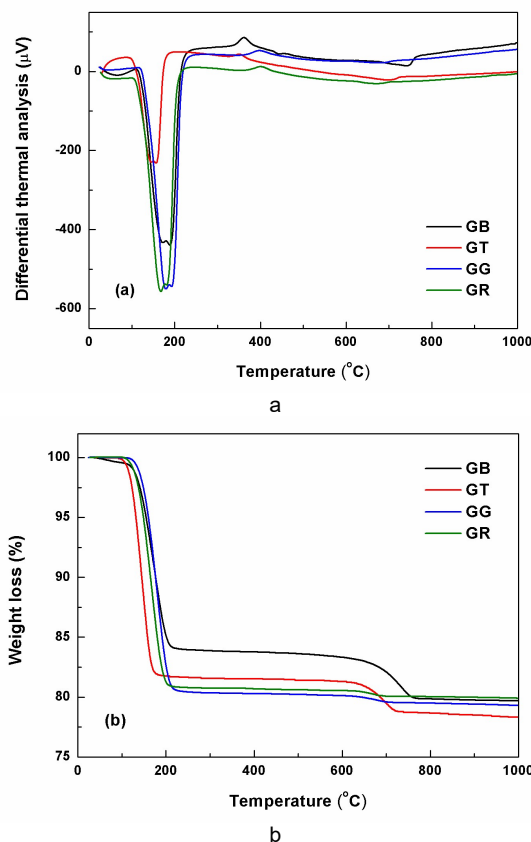


Fig. 1 - Thermal analysis of the four gypsum samples: (a) differential thermal analysis and (b) thermogravimetric analysis / Analiza termică a celor patru probe de ghips: (a) analiza termică diferențială și (b) analiza termogravimetrică

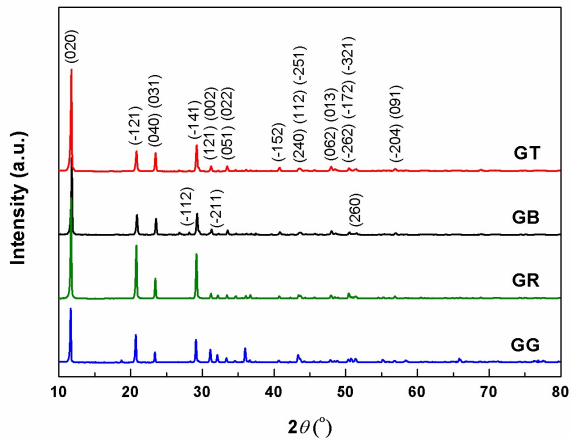


Fig. 2 - XRD patterns of the four gypsum samples / *Analizele de difracție de raze X ale celor patru probe de ghips.*

Fig. 2 shows the XRD patterns of all gypsum specimens. As it can be seen, calcium sulphate hydrate (gypsum) with monoclinic structure and  $I2/c$ - space group (ICDD 00-074-1904) is the only crystalline phase that could be detected with the help of this investigation technique and corresponding software. The position of the diffraction peaks is slightly shifted at higher angles in the case of sample GB, which could be associated with a small concentration of defects (vacancies, interstitials etc.) present in the crystalline network. Moreover, the relative intensities of the diffraction peaks are different as regards the theoretical pattern, suggesting a certain texturing of these materials, namely preferential growth on specific crystallographic directions.

Using Scherrer's formula [16], the average crystallite size of gypsum phase was calculated through mediation on the first three most intense diffraction peaks, as follows: specimen GB - 47 nm, specimen GT - 46 nm, specimen GG - 55 nm and specimen GR - 52 nm. These values could subsequently influence the hydration kinetics of gypsum samples. At a closer look, the specimens with a higher average crystallite size present some additional diffraction peaks with a very low intensity; these features can be well correlated with the results of the thermal analysis, which evidenced a similar behavior for samples GG and GR.

The morphological characteristics of gypsum powders are presented in the SEM images recorded in backscatter mode from Fig. 3. Specimens GG and GR (Figs. 3c and d) are composed of particles with quasi-spherical or polyhedral shape, sometimes with a considerable proportion of micrometric pores, but placed in a relative narrow dimensional spectrum, around few tens of microns. Going to samples GB and GT (Figs. 3a and b), it can be observed that their aspect is completely different, with a finer

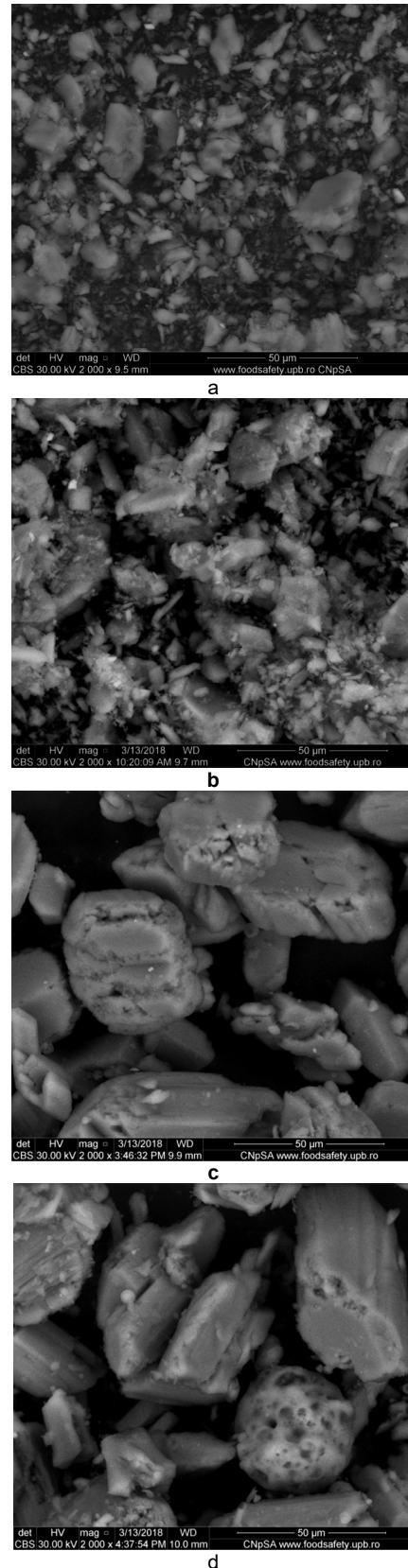


Fig. 3 - SEM images of the four gypsum samples: (a) GB, (b) GT, (c) GG and (d) GR / *Imagini SEM ale celor patru probe de ghips: (a) GB, (b) GT, (c) GG și (d) GR.*

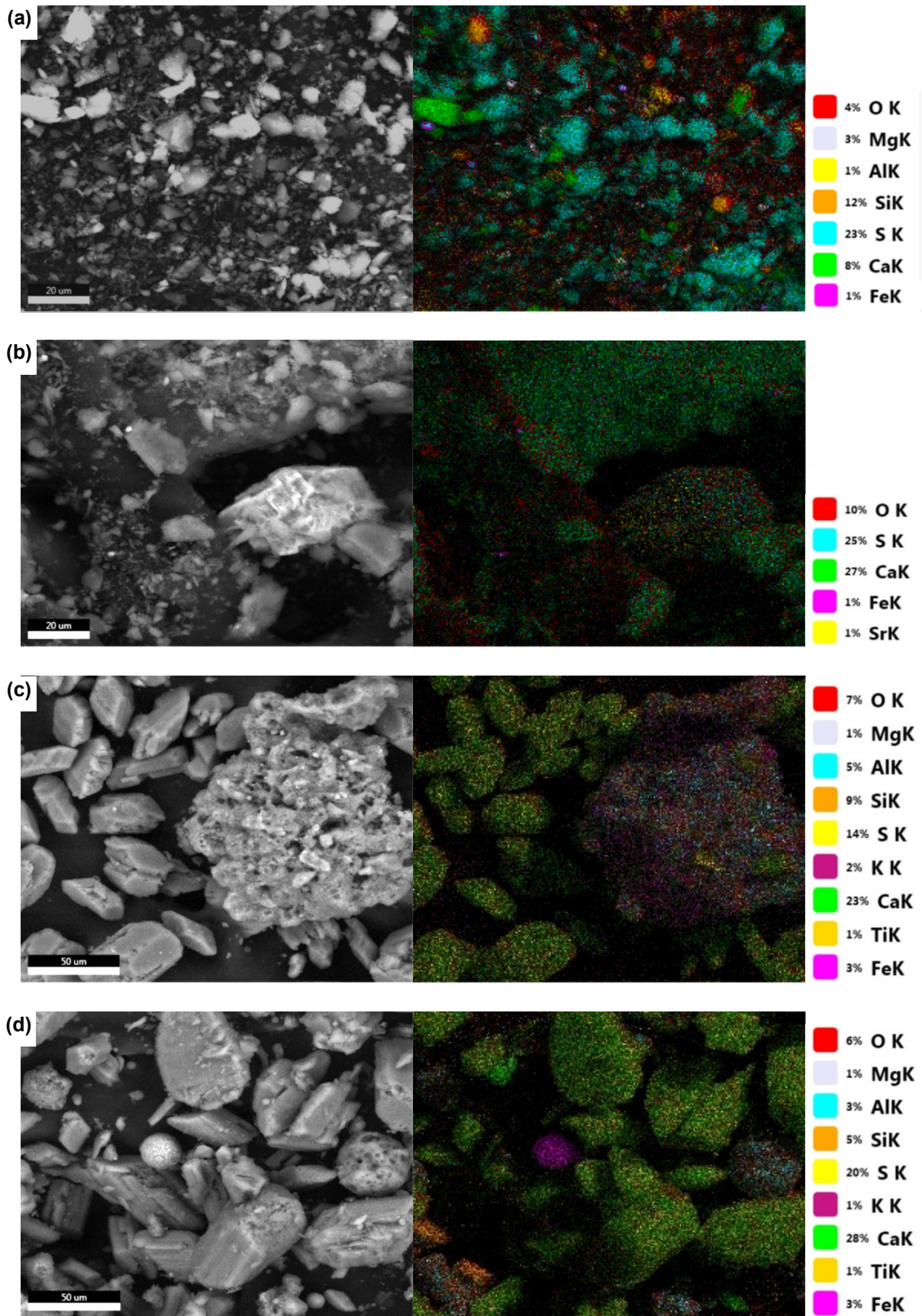


Fig. 4 - SEM images and EDX maps of the four gypsum samples: (a) GB, (b) GT, (c) GG and (d) GR / Imagini SEM și hărțile EDX ale celor patru probe de ghips: (a) GB, (b) GT, (c) GG și (d) GR.

appearance, which could suggest a higher reactivity; the powder consist of both particles with size below 1  $\mu\text{m}$  and much bigger blocks or aggregates.

In order to evaluate the contamination degree, in the conditions of highly non-homogenous samples, each gypsum specimen was approached by EDX mapping, the resulting elemental distributions obtained on selected areas being shown in Fig. 4, together with the SEM images of the same areas. Indeed, samples GG and GR (Figs. 4c and d) present high percentages of foreign elements; usually, the porous particles are the most contaminated especially with Si, Al and Fe. It can be supposed

that these category of particles with modified composition has a glassy nature due to the existence of  $\text{SiO}_2$ , a network former in glass science, but also to the porous and brittle aspect of these structures. As well, specimen GB (Fig. 4a) contains significant percentages of Si and Mg, probably a magnesium silicate, quartz or magnesium carbonate, found together with the gypsum rock. Specimen GT (Fig. 4b) seems to be the cleanest of all, due to the proportions of impurities that are placed below 1 %.

In order to get more information about the particle size distribution of the powders, Fig. 5 presents the typical curves recorded with the help of a laser granulometer, using air as dispersion

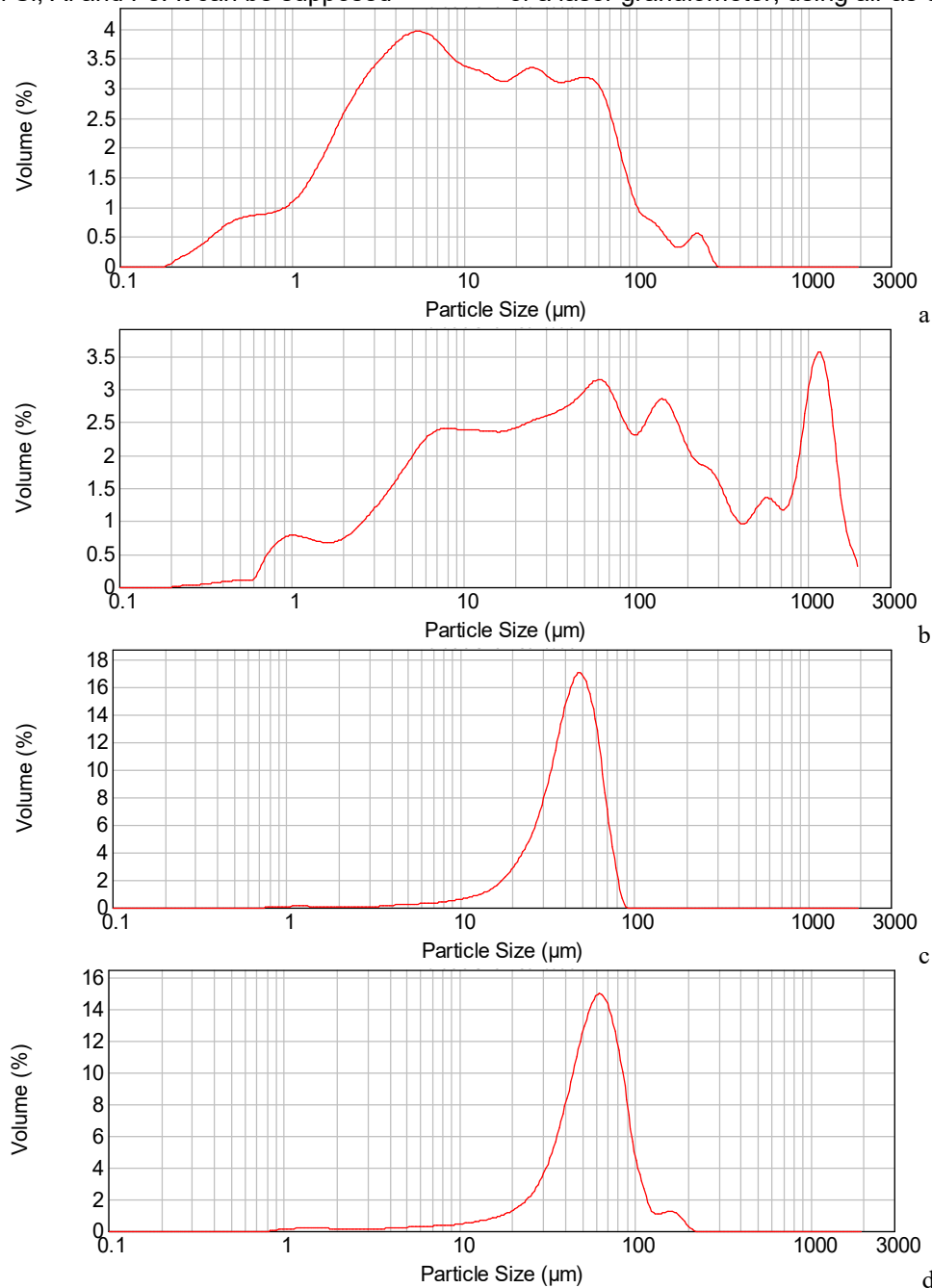


Fig. 5 - Particle size distribution curves of the four gypsum samples: (a) GB, (b) GT, (c) GG and (d) GR / Curbele de distribuție după dimensiune a particulelor pentru cele patru probe de ghips: (a) GB, (b) GT, (c) GG și (d) GR.

medium. Again, there are two typologies: either monomodal or almost monomodal graphical representations with maximum at 50 - 60  $\mu\text{m}$  (GG and GR samples, Figs. 5c and d), or polymodal charts with at least five granulometric fractions overlapped in a continuous spectrum from less than 1  $\mu\text{m}$  to more than 100  $\mu\text{m}$  (GB specimen, Fig. 5a) and 1 mm (GT specimen, Fig. 5b), respectively. Thus, the hydration and hardening behaviour of samples GG and GR is easier to predict and control since the particles have dimensions in a small granulometric range, while in the case of the other specimens the binding properties will be strongly influenced by the powder degree of agglomeration (if the coarse fraction is due to the presence of aggregates that could not be separated) or by the reactivity of large particles (if the coarse fraction is due to the presence of individual entities). However, for sample GB the most abundant fraction is the one centred at 5  $\mu\text{m}$ , while for sample GT is located slightly above 1 mm. The aforesaid findings can be very well correlated with the microstructural properties revealed by the SEM investigation (Fig. 3).

Going to the binding properties, Figs. 6 and 7 display the setting time (initial and final), as well as the flexural strength and compressing strength for five samples prepared with each gypsum powder in different proportions (1, 2, 3, 4 and 5 %). It is obvious that the setting time values, both initial and final, do not present significant variations over a gypsum ratio of 2 %, the small differences being attributed to the measurement uncertainty.

As it was expected, both mechanical parameters (flexural strength and compression strength) increase by extending the hardening period from 2 to 7 and 28 days for all investigated masses. As well, the mechanical properties vary with the gypsum content in the initial stage of hardening (2 days), increasing with gypsum content growth, as a consequence of the decreased rate of interaction between tricalcium aluminate and water. For hardening periods longer than 7 days, the mechanical properties are no longer influenced by the gypsum amount because they no longer depend on the hydration of tricalcium aluminate, but are mainly due to the formation of hydrosilicates.

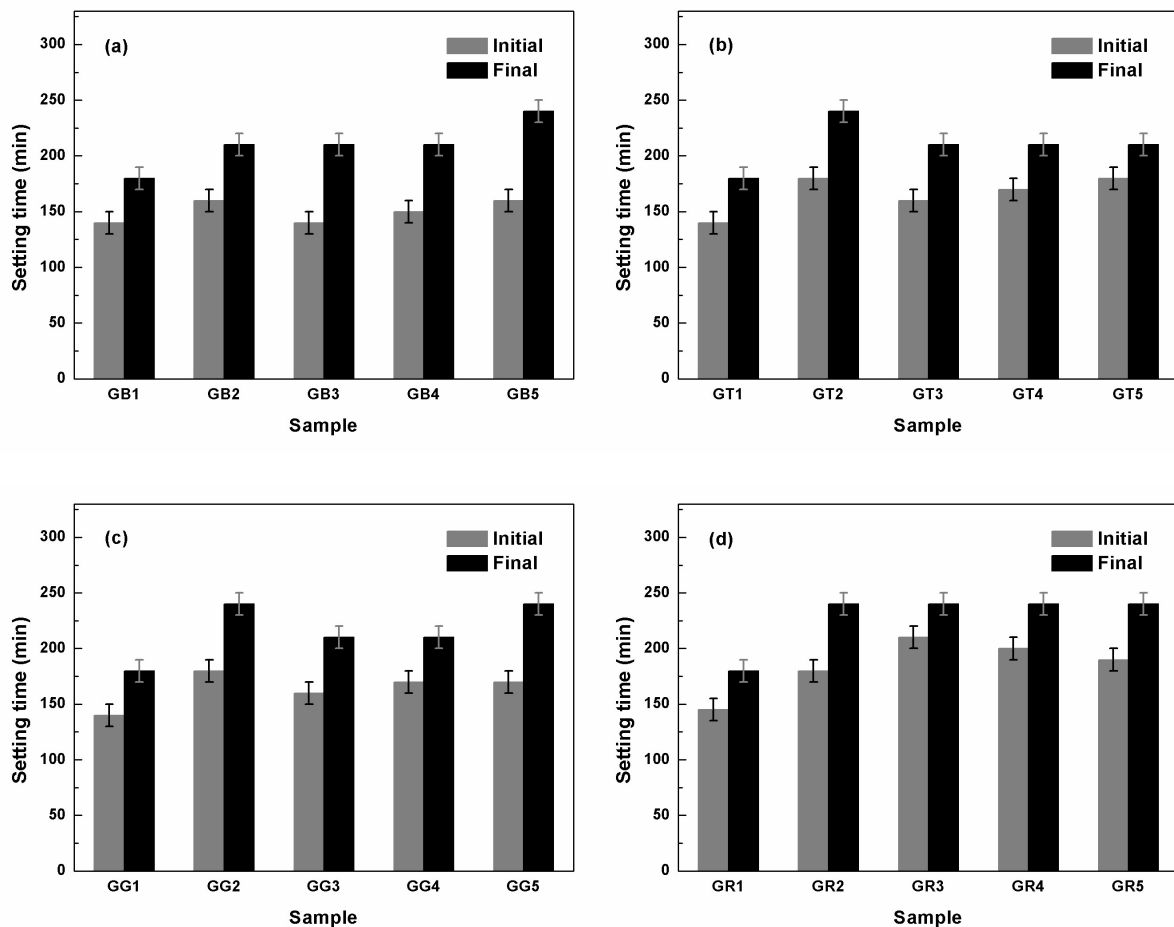


Fig. 6 - Setting time of the four gypsum types: (a) GB, (b) GT, (c) GG and (d) GR / *Timpul de priză pentru cele patru tipuri de ghips: (a) GB, (b) GT, (c) GG și (d) GR.*

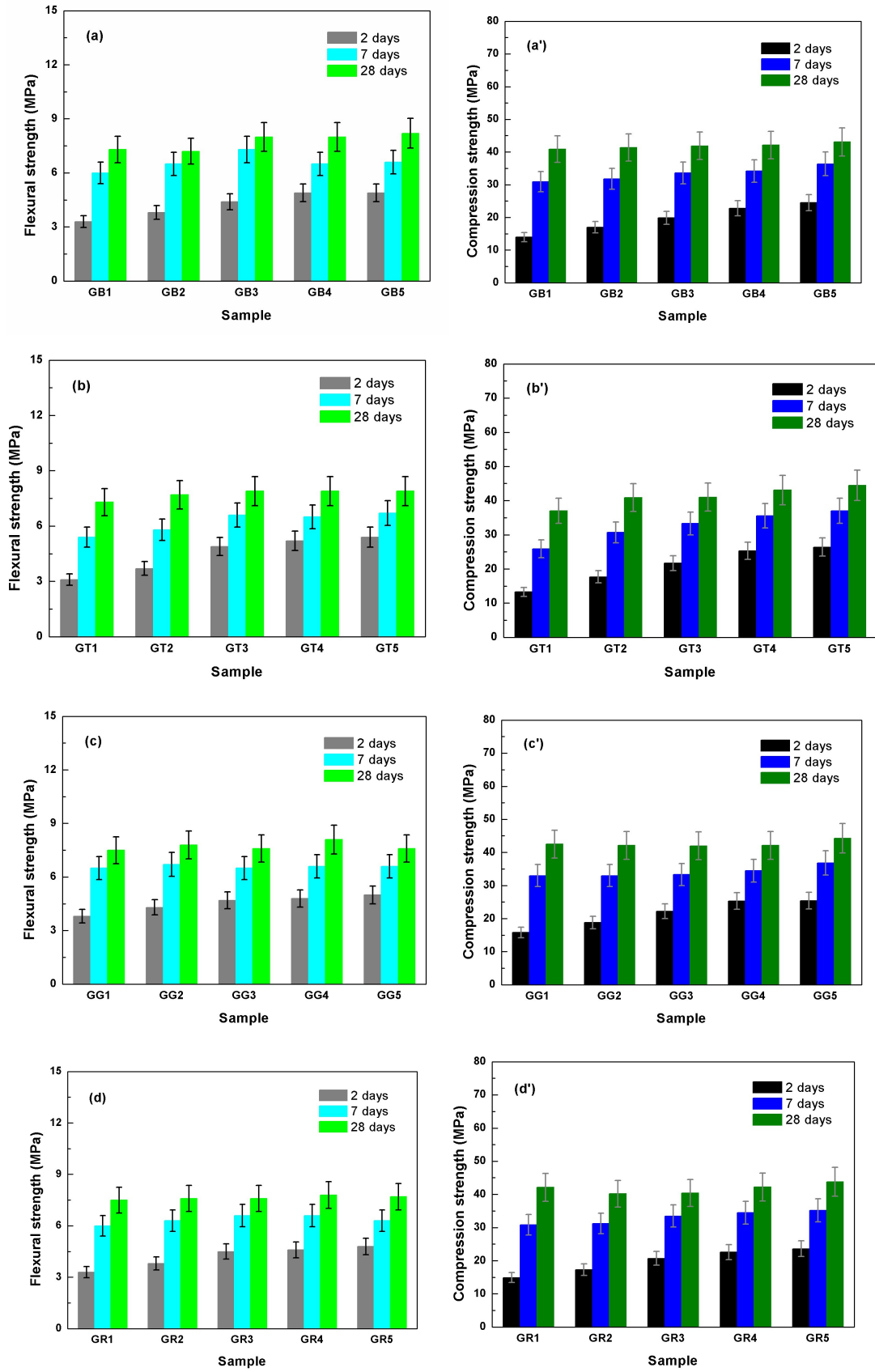


Fig. 7 - Flexural ( $S_f$ ) and compression ( $S_c$ ) strengths at 2, 7 and 28 days of the four gypsum types: (a and a') GB, (b and b') GT, (c and c') GG and (d and d') GR / *Rezistențele la încovoiere ( $S_f$ ) și compresiune ( $S_c$ ) la 2, 7 și 28 zile pentru cele patru tipuri de ghips: (a și a') GB, (b și b') GT, (c și c') GG and (d și d') GR.*

In the case of GT1, the strength values are lower because there is not enough sulphate to react with tricalcium aluminate. In these conditions, the hardening structure of these masses is poorer, as an effect of the heat released during tricalcium aluminate hydration process and conversion of calcium hidroaluminates from hexagonal to cubic symmetry, leading to microcracking. At higher GT proportions, there will be sufficiently sulphate within the system so that tricalcium aluminate to bind in the form of hydrated calcium sulfoaluminate, with beneficial effects on the mechanical strength.

With the exception of GT1, the studied cements are CEM I type and belong to 42.5 N or R resistance class (switching from N to R with gypsum proportion increasing, as a result of better hardening kinetics of tricalcium aluminate).

The following SEM images display some morphologies of the hydration product found in two of the developed mortars, one based on GG type gypsum and the other on GT type gypsum, namely gypsum specimens with different origin. Structures with a fine laced aspect spread over large areas, needle like crystals or thin foils intertwined as porous layers specific to calcium silicate hydrates

(CSH) (Fig. 8a), hexagonal crystals typical of calcium hydroxide (CH) (Fig. 8b), mushroom like architectures developed radially from a starting core characteristic for calcium carbonate (CC) (Fig. 8c), as well as long acicular prism shapes specific to ettringite (Et) (Fig. 8d) can be clearly observed and considered results of the hydration and hardening processes [17].

The maximum value of  $SO_3^-$  content is lower than 3.5 % (Fig. 9), value which is in accordance with cement standards and literature data [11, 18]. The exceeding of this value leads to decreasing of mechanical properties and dramatic changes in hydration processes. As it can be seen in [18], hydration kinetic and porosity distribution and pore dimensions depends on  $SO_3^-$  content and reactivity of  $SO_3^-$  sources. Our results indicate a better reactivity of gypsum from waste sources than gypsum from natural sources with a soft effect upon mechanical properties, at least up to seven days. This advantage influences the mechanical properties at 28 days, samples with gypsum from waste showing maximum mechanical strengths starting with 1 %.

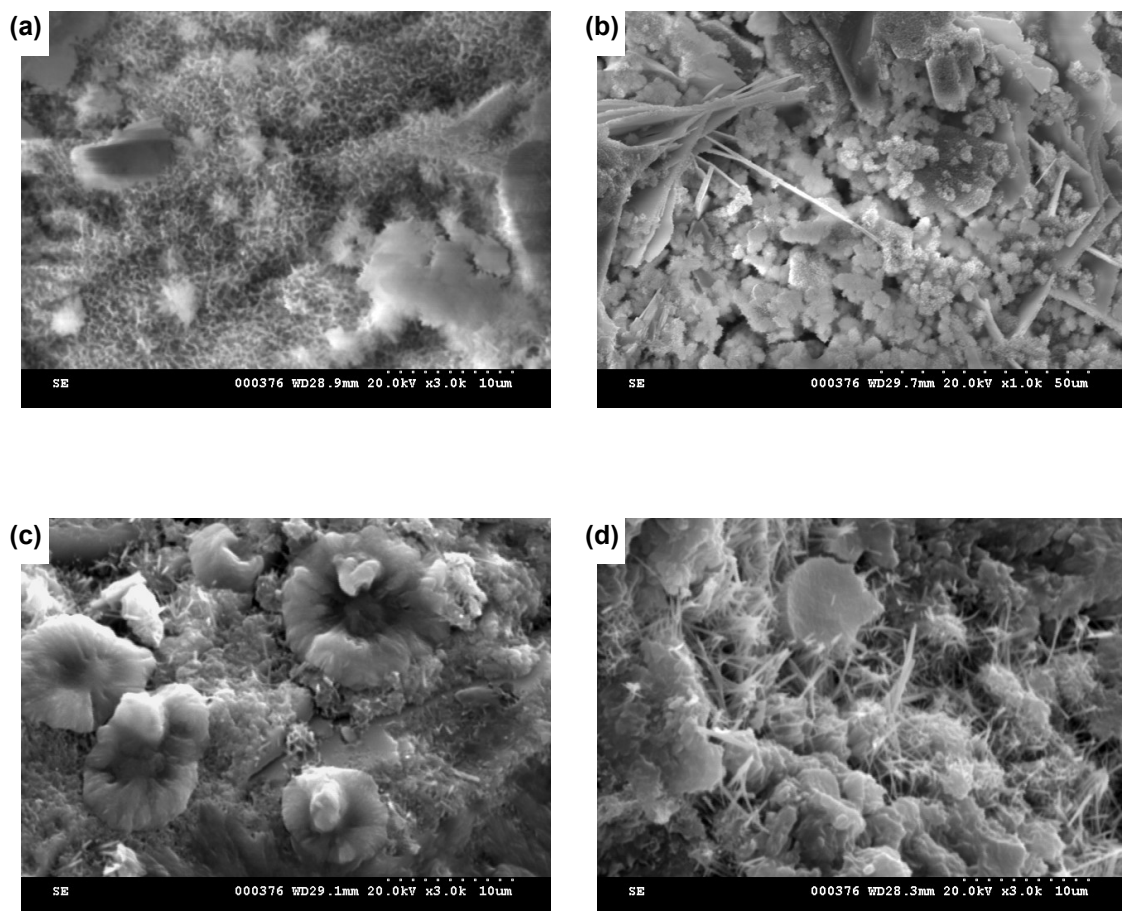


Fig. 8 - SEM images of some mortars prepared with 1 % GG (a and b) or GT (c and d) type gypsum, hardened for 28 days / Imagini SEM ale unor mortare preparate cu 1 % ghips de tip GG (a și b) sau GT (c și d), întărite 28 de zile.

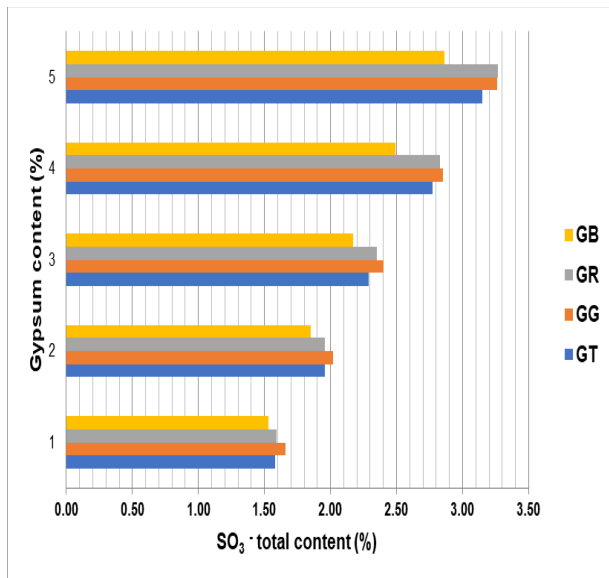


Fig. 9 - Total content of  $SO_3^-$  depending on setting retarder in proportions between 1 and 5 % / *Conținutul total de  $SO_3^-$  în funcție de întăzietorul de priză în proporții între 1 și 5 %.*

#### 4. Conclusions

Four types of gypsum, two with natural origin and two resulted as industrial waste, were investigated from physicochemical point of view in order to understand their influence on the properties of portland cement based mortars, when employed as setting retarder in proportions between 1 and 5 %. The natural samples are contaminated to a lesser extent, but present a large, polymodal particle size distribution, while the synthetic ones contain small quantities of secondary phases and a monomodal particle size distribution, centred at 50 - 60  $\mu m$ . The derived mortars were evaluated in terms of setting time and mechanical properties, which revealed the influence of gypsum contents below 2 % when it comes to the setting time and the beneficial effect of gypsum on the flexural strength and compression strength for all investigated proportions of retarder.

The replacement of natural gypsum can be done in any concentration with gypsum from industrial waste, between 1 and 5 %, having also a small advantage regarding the obtaining of good mechanical properties for low  $SO_3^-$ .

#### Acknowledgements

The SEM analyses on samples were possible due to EU-funding grant POSCCE-A2-O2.2.1-2013-1, Priority direction 2, Project No. 638/12.c03.2014, Code SMIS-CSrNR 48652.

#### REFERENCES

1. T. Adams, P. Amaya, D.P. Bentz, J.D. Bittner, A. Bittner, G.M. Blythe, L.J.N. Bradley, T. Butalia, N.E. Carriker, J. Castleman, L.J. Csetenyi, S. Dai, J.L. Daniels, D. French, U.M. Graham, J. Groppo, D. Harris, K.R. Henke, B. Hensel, J.C. Hower, F.J. Hrach, R. Jewell, R. Jones, J. Jow, R.A. Kruger, K.J. Ladwig, L. Lemay, A. Lewis, S. Liu, M.J. McCarthy, R. Minkara, H.W. Nugteren, K. Radloff, T. Robl, R.V.R. San Nicolas, L.L. Sutter, M. Thomas, J.S.J. van Deventer, B. Walkley, C.R. Ward, W. Wolfe, Coal Combustion Products, Woodhead Publishing, 2017.
2. R. Lisnic, S.I. Jinga, Study on current state and future trends of flue gas desulphurization technologies: A review, Romanian Journal of Materials, 2018, **48** (1), 83.
3. P. Cordoba, Status of Flue Gas Desulphurisation (FGD) systems from coal-fired power plants: Overview of the physico-chemical control processes of wet limestone, Fuel, 2015, **144**, 274.
4. Flue gas desulphurisation wet limestone-gypsum process, KC Cottrell Co., Ltd., 2016.
5. G. Carmi, M. Schutt, Increasing the use of synthetic gypsum in the cement industry, IEEE-IAS/PCA Cement Industry Technical Conference, 2017, Calgary, AB, Canada.
6. F. Clamp, Trials for the use of recycled gypsum in cement manufacture, Project code: PBD022-001, Jacobs Engineering UK Ltd., 2008.
7. R.P. Borg, C. Briguglio, V. Bocullo, D. Vaiciukyniene, Preliminary investigation of geopolymer binder from waste materials, Romanian Journal of Materials, 2017, **47** (3), 370.
8. J.H. Potgieter, S.S. Potgieter, R.I. McCrindle, A comparison of the performance of various synthetic gypsums in plant trials during the manufacturing of OPC clinker, Cement and Concrete Research, 2004, **34** (12), 2245.
9. G. Tzouvalas, G. Rantis, S. Tsima, Alternative calcium-sulfate-bearing materials as cement retarders, Part II. FGD gypsum, Cement and Concrete Research, 2004, **34** (11), 119.
10. xxx, SR EN 197-1, Cement, Part 1: Composition, specifications and conformity criteria for common cements, 2011.
11. xxx, SR EN 196-2, Methods of testing cement, Part 2: Chemical analysis of cement, 2013.
12. xxx, SR EN 196-3, Methods of testing cement, Part 3: Determination of setting time and soundness, 2017.
13. xxx, SR EN 196-1, Methods of testing cement, Part 1: Determination of strength, 2016.
14. L. Scheinherrova, M. Dolezelova, J. Havlin, A. Trnik, Thermal analysis of ternary gypsum-based binders stored in different environments, Journal of Thermal Analysis and Calorimetry, 2018, **133** (1), 177.
15. D.N. Todor, Thermal Analysis of Minerals, Technical Publishing House, București, 1972.
16. F.T. Muniz, M.A. Miranda, C. Morilla Dos Santos, J.M. Sasaki, The Scherrer equation and the dynamical theory of X-ray diffraction, Acta Crystallographica A, 2016, **72** (3), 385.
17. D.H. Campbell, Microscopical Examination and Interpretation of Portland Cement and Clinker, Second edition, Portland Cement Association, 1999.
18. M. Zajac, J. Skocek, A. Muller, M.B. Haha, Effect of sulfate content on the porosity distribution and resulting performance of composite cements, Construction and Building Materials, 2018, **186**, 912.

\*\*\*\*\*